Proceedings of the
Annual Stability Conference
Structural Stability Research Council
San Antonio, Texas, March 21-24, 2017

Lateral Torsional Buckling of Butterfly-Shaped Shear Links

Alireza Farzampour [1], Matthew Eatherton [2]

Abstract
A promising type of hysteretic damper used for seismic energy dissipation consists of a set of butterfly-shaped links subjected to shear deformations. Prior research has been conducted on shear panels with straight links, also referred to as steel slit panels or slit steel plate shear walls. Butterfly-shaped links have been proposed more recently to better align bending capacity with the shape of the moment diagram. The links have linearly varying width between larger ends and a smaller middle section. These links have been shown in previous tests to be capable of substantial ductility and energy dissipation, but can also be prone to lateral torsional buckling. In this article, the lateral torsional buckling of a butterfly-shaped link subjected to shear loading is conceptualized, and differential equations governing the links' buckling behavior are formulated. The differential equations are numerically solved for a useful range of link geometries. The resulting critical moment, and related critical shear, are provided in a useful format for use in butterfly link design. Strategies for controlling lateral torsional buckling in butterfly links are recommended and are validated through comparison with finite element models

1. Introduction

Earthquake resistant structural design relies on the ductile behavior of the structural members to create inelastic drift capacity and energy dissipation. If these ductile members are also replaceable, they are sometimes referred to as structural fuses because they yield and thus limit the earthquake forces applied to the surrounding structure (Vargas and Bruneau 2006). The fuses are used to protect the surrounding structure from damage and then be accessible and easily replaceable after a major event (Martinez-Rueda 2002). There are many forms of structural elements with adequate ductility and energy dissipating capability which could be implemented as structural fuses.

Several studies have indicated that steel plates having slit or butterfly-shaped cut-outs have advantages for use in structural fuses. Butterfly-shaped links (Fig. 1) better align moment capacity with the shape of the moment diagram leading to efficient implementation of the steel with distributed yielding. The planar geometry of the butterfly-shaped links make them applicable for space-constrained applications as well (Ma et al. 2011).

[1] Graduate Research Assistant, Virginia Tech, <afarzam@vt.edu>
[2] Associate Professor, Virginia Tech, <meather@vt.edu >

Shapes similar to the butterfly have been used in the past, but with out-of-plane orientation. These out-of-plane links were previously used in tapered yielding plates to dissipate energy and impose higher ductility of structures in moment resisting frames. (Whittaker et al. 1991, Tsai et al. 1993, Asselin et al. 2012, Chan and Albermani 2008). These links have been used in a variety of passive control energy-dissipating systems (Tsai et al. 1993, Martinez-Rueda 2002), as well as link beams to have a better distribution of yielding in the system (Aschheim and Halterman 2002).

Previous testing has shown that butterfly-shaped links can experience lateral torsional buckling (LTB) which can lead to loss of strength and stiffness (Ma et al. 2011). Steel butterfly links as shown in Fig. 1 are analytically and numerically investigated in this study. Differential equations are developed first, and mathematical solutions for such equations are found. The differential equation associated with the reversed moments applied to the ends of the butterfly section assume that the moment along the link length varies linearly. In addition, the effect of torsional moment on buckling is considered in developing the governing equations. Finite element (FE) models are then used to verify the results and examine both the elastic buckling and inelastic limit states.

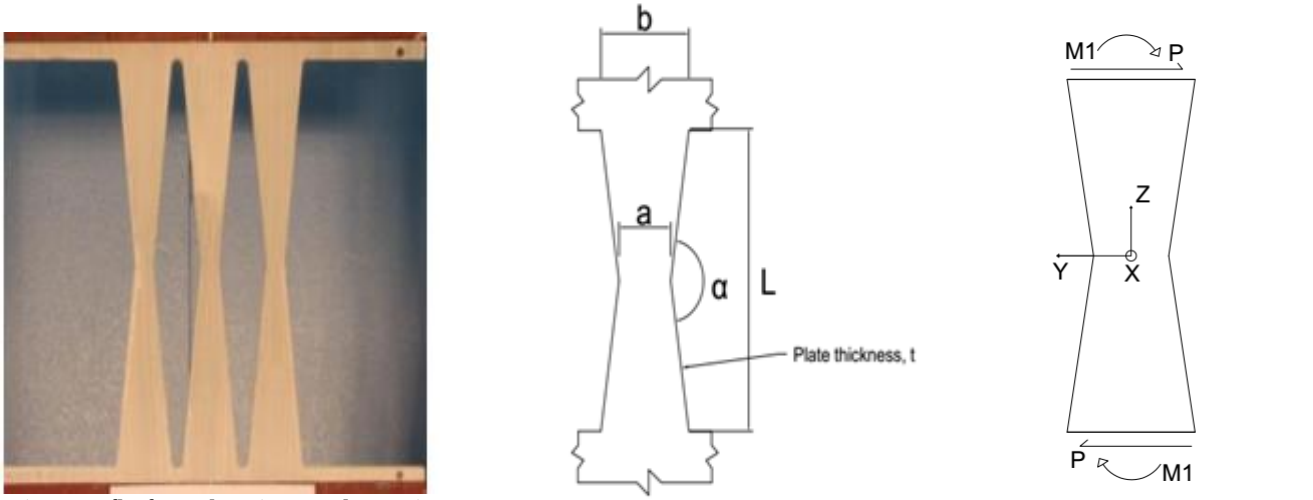

a) Butterfly fuse plate (Ma et al. 2011) b) Butterfly link geometry c) Loading and coordinate axes

Figure 1: The butterfly fuse, link geometry and loading

2. The governing differential equation for butterfly-shaped links

In this section, a differential equation is formulated with twist about the longitudinal axis as the variable. It is noted that the cross section is rectangular and relatively thin compared to its width. Fig. 2(a) indicates the local axes from top view, and Fig. 2(b) represents the section view, as well as showing the situation of local axes with applied moment on the section.

According to Fig. 2, the following differential equations could be derived based on assumptions associated with the governing differential equations of equilibrium (Timoshenko 1938). It is assumed that the link is free to warp which is a common assumption in lateral torsional buckling analysis of a beam (Timoshenko 1938). It is noted that only uniform torsion (or St. Venant's) is

applied to the section and the ends are free to warping. Eq. 1, Eq. 2 are developed to evaluate the moments about the local axes considering the related deformation variable.

Since the objective is to derive the critical buckling moment in terms of M as shown in Fig. 1, the local moments are put in terms of M. From the figure at the top of Fig. 2a, and considering small rotation values, the projection of M on local axis, ζ, would result in Eq. 3. To derive Eq. 3, the moment is projected on the local axis considering the angles between them (top of Fig. 2a). It is noted that u' is assumed small; therefore, the *sine* of a term having u' would be approximately equal to u' itself.

$$EI_y u'' = M_\eta = M\sin\beta \tag{1}$$

$$M\sin\beta \approx \beta M \,(For\ small\ values\ of\ \beta) \tag{2}$$

$$M_\zeta = -\cos\left(\pi - \left[\frac{\pi}{2} + u'\right]\right)M = -Sin(u')M \approx -u'M \tag{3}$$

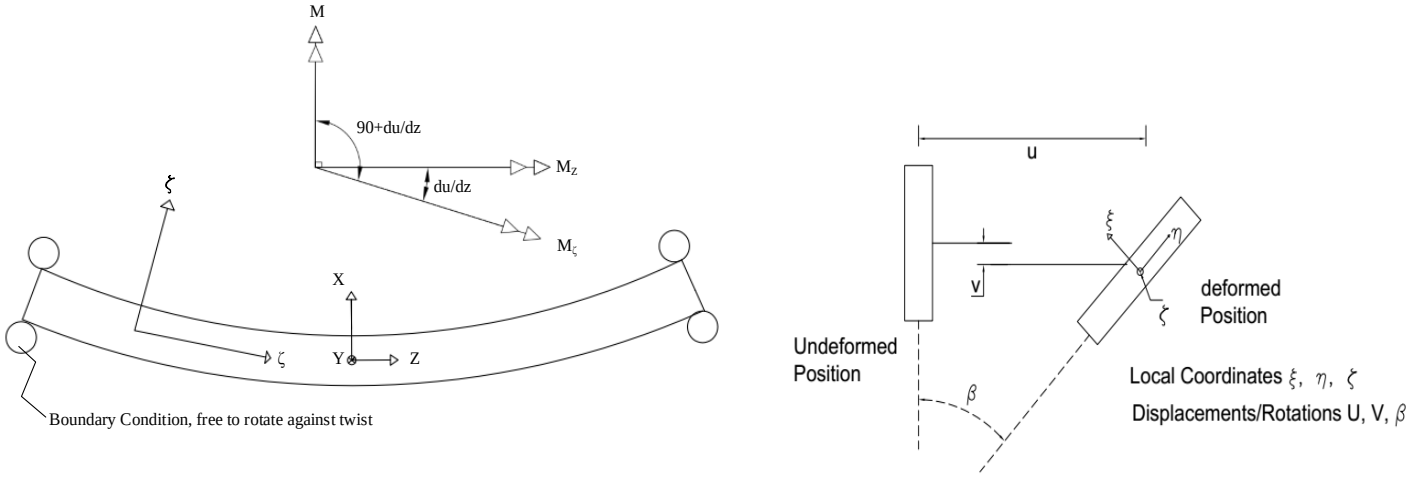

a) Top view b) Section view

Figure 2: Defining local axes and displacement variables

The variables u and v are the horizontal and vertical displacements as indicated in Fig. 2(b), β is the rotation about the longitudinal axis (twist), and β' is derivative of rotation with respect to z. GJ is the torsional rigidity of the strip along the butterfly link. In addition, EI_y is the flexural rigidity about the weak axis. The width of the butterfly link, w, could be formulized as Eq. 4 which is valid for 0<z<L/2.

$$w(z) = a + 2(b-a)z/L \tag{4}$$

The angle of twist is small; therefore, $\sin\beta$ and $\cos\beta$ are approximately equal to β and 1, respectively. According to Roark's book (Young and Budynas 2002), the equation of torsional constant, *J*, of a rectangular section is indicated in Eq. 5.

$$J = \left(\frac{w}{2}\right)\left(\frac{t}{2}\right)^3\left[\frac{16}{3} - 3.36\frac{t}{w}\left(1 - \frac{t^4}{12w^4}\right)\right] \tag{5}$$

According to Fig. 3(a), the moment distribution is formulated as given in Eq. 6, where M_1 is the end flexural moment at the end of the butterfly link. The derivative of the moment along the butterfly link length, *M'*, is obtained to be used as an input for the differential equations.

$$\begin{aligned} M &= M_1 - P(z + l/2) \\ M' &= -P \end{aligned} \tag{6}$$

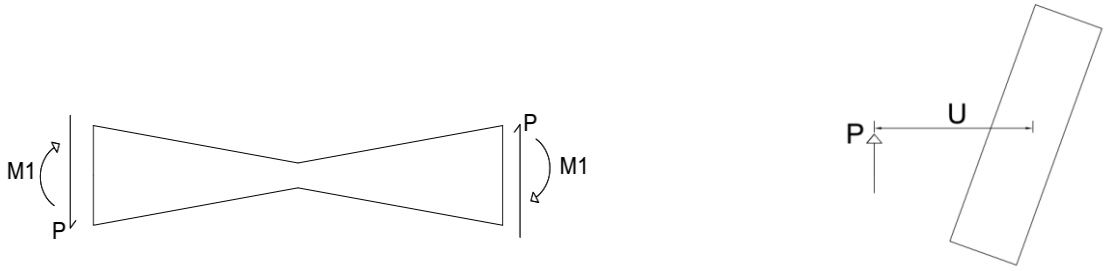

a) The butterfly link from the side view

b) The section view after buckling

Figure 3: The butterfly link after buckling

The torsional moments can then be summed for an arbitrary section along the length to obtain the following differential equation:

$$GJ\beta' = -Mu' - Pu + M_{end} \tag{7}$$

The term on the left side of the equation is the internal torsional moment at the section. The first term on the right side is the torsional moment, M_{β}, due to the primary moment, *M*, given in Eq. 3. The second term on the right side of the equation is the torsional moment due to the load *P* acting at a deflection, *u*, as shown in Fig. 3b. The last term, M_{end}, is the fixed torsional moment at the end.

Taking the derivative of Eq. 7 leads to Eq. 8. It is noted that *J* is a function of *z*, so the left side is not simplified beyond what is shown in Eq. 8. Substituting the term $M' = -P$ (from Eq. 6) causes the first and last terms on the right side to cancel out, and substituting Eq. 1 leads to Eq. 9:

$$\left(GJ\beta'\right)' = -M'u' - Mu'' - Pu' \tag{8}$$

$$\left(GJ\beta'\right)' = -\frac{\beta M^2}{EI_y} \tag{9}$$

From the moment loading distribution (Eq 6) along the length of the beam, the moment for the right half of the link can be rewritten as:

$$\begin{aligned} P &= \frac{2M_1}{L} \\ M &= -\frac{2M_1}{L} z \end{aligned} \tag{10}$$

Therefore, Eq. 10 could be rewritten as follows, which is the governing differential equation regarding butterfly-shaped link lateral torsional buckling.

$$\left(GJ\beta'\right)' + \frac{4M_1^2}{l^2} z^2 \frac{\beta}{EI_y} = 0 \tag{11}$$

3.1 Solution assessment using parameter non – dimensionaliziation for governing differential equations

In order to get all the differential equations in appropriate format to be solved in Mathematica, it is useful to reformulate the parameters to be non-dimensional first. A way to do so is to divide all the dimensions by the length of the link. In what follows, each equation is non-dimensionalized with regard to each parameter as indicated in Eqs 12-15. The nondimensionalized versions of Eqs. 4 and 5 are given by Eqs. 13 and 14. Poisson's ratio is assumed equal to 0.3.

$$\begin{gathered} A = a/L \quad B = b/L \quad G = E/2.6E \\ \Omega = M_1/EL^3 \quad K = \frac{J}{L^4} \quad Z = z/L \quad T = t/L \end{gathered} \tag{12}$$

$$W\left(Z\right) = A + \left(2\left(B - A\right)Z\right) \tag{13}$$

$$K = \frac{1}{3}T^3 W\left(1 - \left(\frac{0.63T}{W}\right)\left(1 - \left(\frac{T}{W}\right)^4\right)\right) \tag{14}$$

$$\mathrm{I_y} = \frac{1}{12}\mathrm{t^3 w} \rightarrow \phi_y = \frac{1}{12}T^3 W \tag{15}$$

Therefore, the non-dimensionalized version of the differential equation could be written as Eq. 16 which is valid for 0<z<1/2.

$$\left(\frac{K\beta'}{2.6}\right)' + 4\Omega^2 Z^2 \frac{\beta}{\phi_y} = 0 \tag{16}$$

3.2 Solving the Differential Equation Using Mathematica implementing the shooting method:
The non-dimensionalized differential equation from the previous section was input into the software Mathematica. The resulting buckling modes represented by the twist angle, β, can be either symmetric or anti-symmetric. The symmetric mode with no nodes will give the lowest buckling moment (i.e., the critical moment).

Since the problem is linear and homogeneous, one can choose an arbitrary value for β(0). The shooting method is used to solve the differential equation, in which a guessed value would be assigned to the moment, and the program varies it automatically until the boundary condition at z equal to 0.5 is satisfied. If the plot of β(z) looks like a symmetric buckling mode with no nodes (e.g. Fig. 4.), the result is taken as the critical moment. If not, the initial guess for moment is revised until a symmetric buckling mode is obtained.

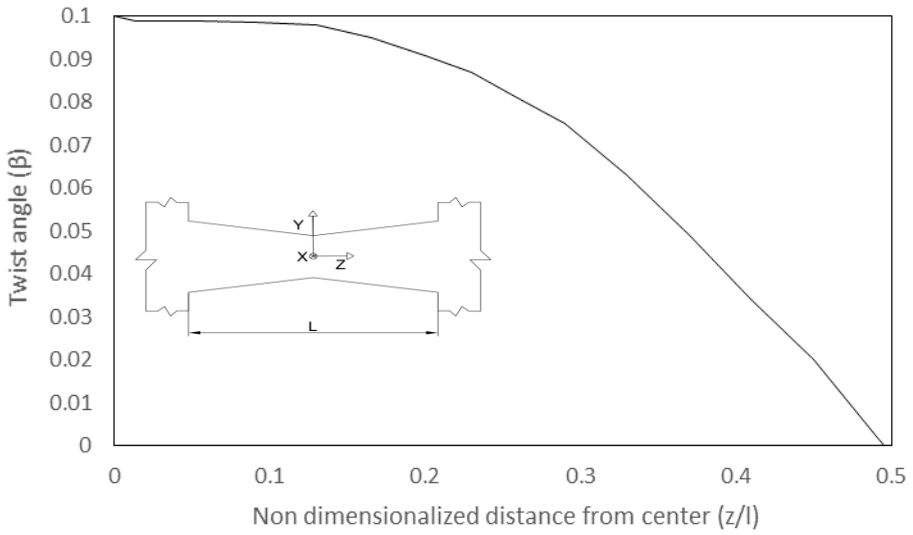

Figure 4: The first mode for a symmetric mode with assumptions of β'(0) = 0 and β(0.5) = 0

Before presenting results for the critical buckling moment, inelastic limit states are discussed. Two inelastic limit states, namely plastic shear yielding and plastic flexural hinging, limit the strength of butterfly links. The domination of each mode depends on the geometry of the links. Eq. 17 gives the end moment corresponding to shear yielding at the middle of the butterfly link based on the Von Mises yielding criteria assuming that the middle section is plastified. The end moment associated with plastic flexural strength is calculated based on procedures used by Ma et al. (2011) assuming a ratio a/b=1/3 which results in plastic flexural hinging at the quarter points of the links as indicated in Eq. 18. Eq. 19 and Eq. 20 indicate the non-dimensionalized version of Eq. 17 and Eq. 18, respectively.

$$M_P^{shear} = \frac{at(\sigma_y / \sqrt{3})\, l}{2} \tag{17}$$

For flexure we have to sue the capacity design concept:

$$M_p^{flexure}=2a^2t\sigma_y \quad (\text{for } \frac{a}{b}=\frac{1}{3}) \tag{18}$$

$$\frac{M_P^{shear}}{El^3}=\frac{AT(\sigma_y/\sqrt{3})}{2E} \tag{19}$$

$$\frac{M_p^{flexure}}{El^3}=\frac{2A^2T\sigma_y}{E} \quad (\text{for } \frac{a}{b}=\frac{1}{3}) \tag{20}$$

Fig. 5a shows the plastic capacity and lateral torsional buckling critical moment for a butterfly link with a/b=1/3, t/L=0.01, σ_y is yielding stress (300 MPa). Fig. 5b shows the results for a thicker plate with t/L=0.03. It is shown that for all thin plate configurations (t/L=0.01) except the least wide configuration (b/L=0.1), LTB is the governing limit state. For thicker plates (t/L=0.03 as shown in Fig 5b), it is shown that plastic section capacity leads to the smallest moment and thus controls the moment strength. In addition, Fig. 5b shows that the narrower links (smaller b/L) experience flexural hinging and wider links experience shear yielding.

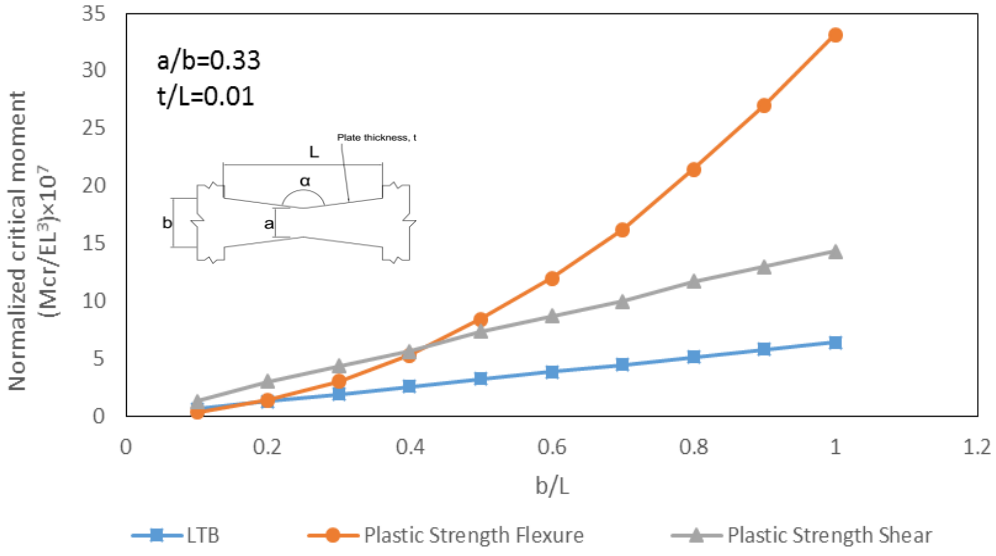

a) Butterfly link with a/b =0.33, t/L=0.01, and L=1m

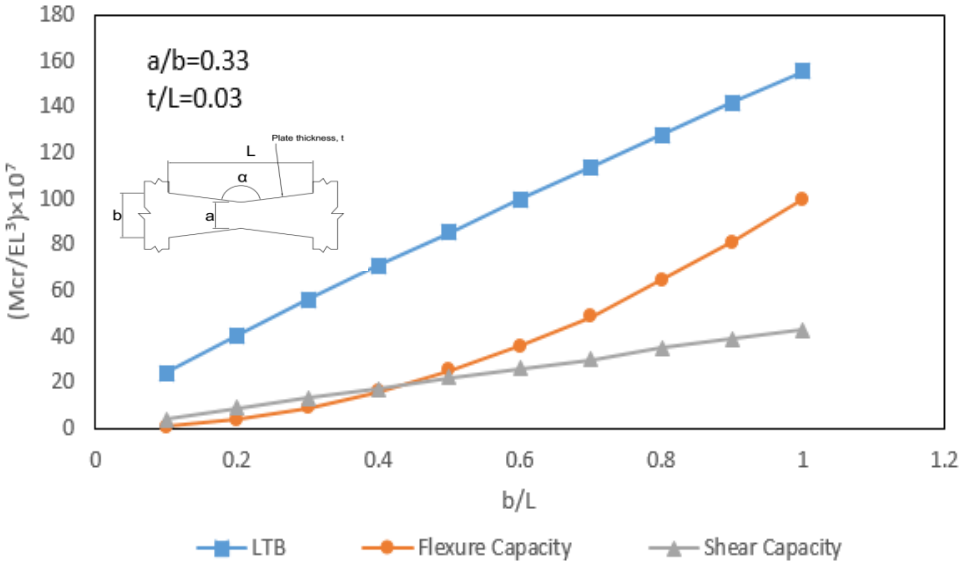

b) Butterfly link with a/b =0.33, t/L=0.03, and L=1m

Figure 5: The capacity and LTB curves

4. Comparison of the Elastic results in Finite Element Analysis software

In this section, the links are modeled in the FE software ABAQUS to verify the analytical solutions generated from solving the governing LTB differential equation as well as plastic strength equations. For each of the link geometries with a/b=1/3, t/L=0.01 or 0.03, link length L=1m and specified b/L, a model was constructed (Fig. 6) and subjected to monotonically increasing lateral displacement along the top edge using an explicit solver. The boundary conditions are fully fixed constraints at the bottom edge, and the vertical as well as out of plane displacement are fixed at the top edge of the links. The mesh sensitivity analysis is conducted but not shown here. The approximate mesh size of 30mm is implemented as represented graphically in the inset of Fig. 6.

A four-node reduced integration element (labeled as S4R in ABAQUS) is chosen as a suitable element type to obtain buckling and the spread of inelasticity (e.g. Farzampour et al. 2015). The initiation of buckling was obtained from the shear force vs. lateral displacement response as shown in Fig. 6. Fluctuations in shear force occurred during the explicit analysis and were correlated with a slight reduction in stiffness and substantial increase in out-of-plane displacement, labeled as values for U in Fig. 6. These fluctuations in shear force were therefore taken as indicating the initiation of the buckling. In Fig6 , δ^{max} indicates the maximum out of plane displacement in the link.

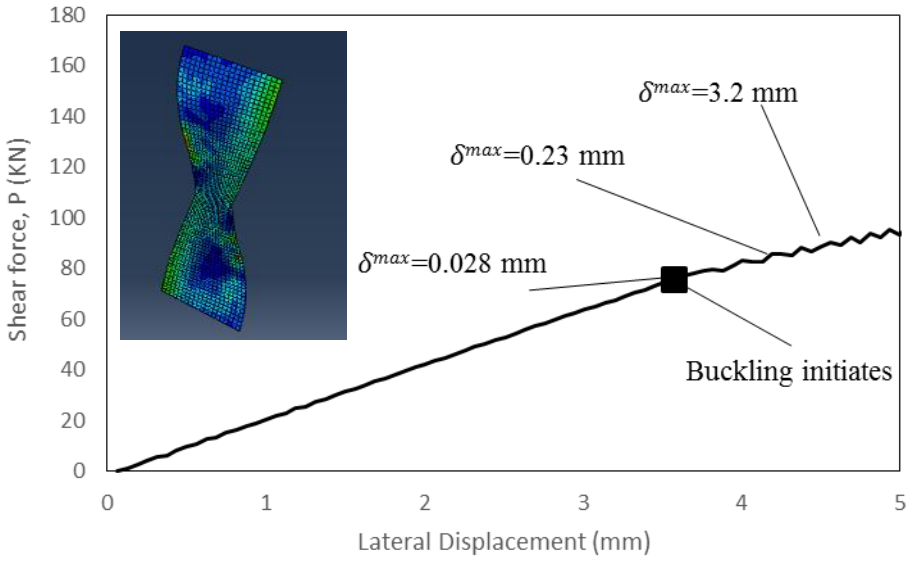

Figure 6: The meshed butterfly-shaped link elastic response for a/b=0.33, b/L=0.3, t/L=0.01, L=1m (U is out-of-plane displacement indicating buckling phenomenon)

First, the FE models were run with elastic material constitutive model to examine elastic lateral torsional buckling. The shear load at buckling was obtained as described above and the associated moment was calculated as given in Table 1. Fig. 7 indicates the comparison between computational simulation and analytical equations. The associated critical moment initiating the lateral torsional buckling of the link is calculated. Table 1 indicates an average of 3.2% difference between the estimation of LTB of butterfly links by solving the general differential equations and the FE model results.

Table 1. Comparison of ABAQUS results with Mathematica

b/L	a/b	t/L	ABAQUS		Mathematica		error%
			P (N)	Moment (kN.m)	Moment × 10^7 (Non-dimen.*)	Moment (kN.m)	
0.1	0.3	0.01	25.2	12.6	0.6	13.4	5.8
0.2	0.3	0.01	55.5	27.7	1.3	28.0	1.0
0.3	0.3	0.01	79.0	39.5	1.9	41.9	5.9
0.4	0.3	0.01	105.2	52.6	2.5	55.9	5.8
0.5	0.3	0.01	139.3	69.7	3.2	70.9	1.7
0.6	0.3	0.01	158.6	79.3	3.8	84.4	6.0
0.7	0.3	0.01	197.9	98.9	4.5	98.3	0.6
0.8	0.3	0.01	228.1	114.1	5.1	113.0	1.0
0.9	0.3	0.01	261.7	130.8	5.8	126.9	3.1
1.0	0.3	0.01	285.1	142.6	6.4	140.8	1.3

*Non-Dimensionlized Moment equal to M_{cr}/El^3

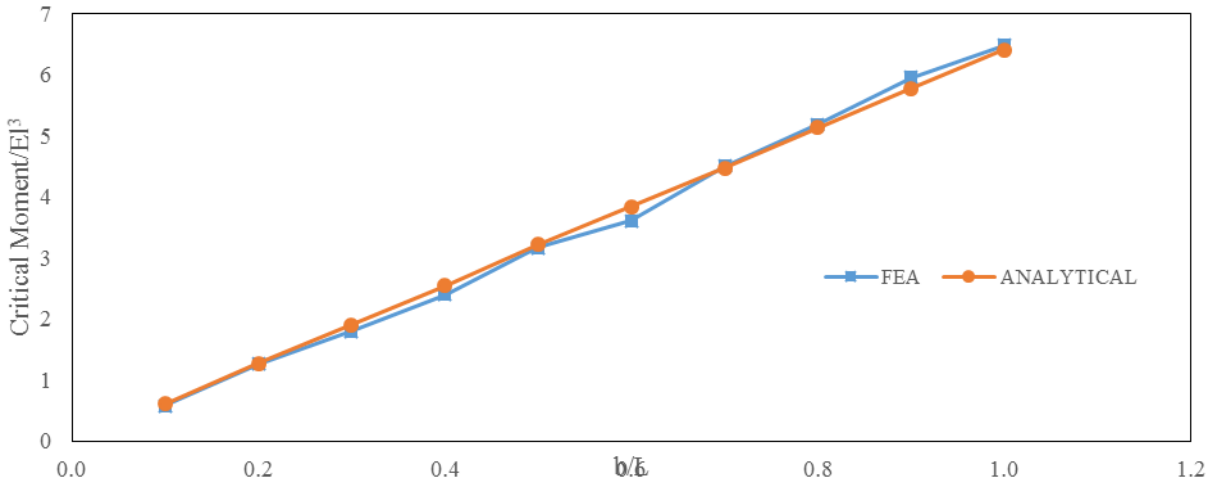

Figure 7: Comparison of buckling differential equations' results with elastic buckling FE models for t/l=0.01

5. Comparison of the Inelastic results in Finite Element Analysis software

In this section, the links are modeled in the FE software ABAQUS with inelastic material constitutive law to compare moments associated with inelastic limit states with proposed equations for flexure and shear capacity. Fig. 8 indicates three lines representing the LTB moment capacity from the differential equation and plastic moment capacity for shear and flexure. The circles indicate the initiation of the buckling while the squares represent the ultimate strength of the link. The models capture the domination of elastic lateral torsional buckling capacity of thinner links. In addition, the FE models capture the plastic shear and plastic flexural capacity for thicker butterfly links (Fig. 8b). Fig. 8b does not show circles associated with buckling in the FE model because significant out-of-plane buckling was not observed. The elastic lateral torsional moment buckling of the links are shown in an inset of Fig. 8b to show how large the elastic lateral torsional buckling moment is related to the plastic moments for thicker plates (Fig. 8b). In general, the FE results are within 3% of the predicted analytical values.

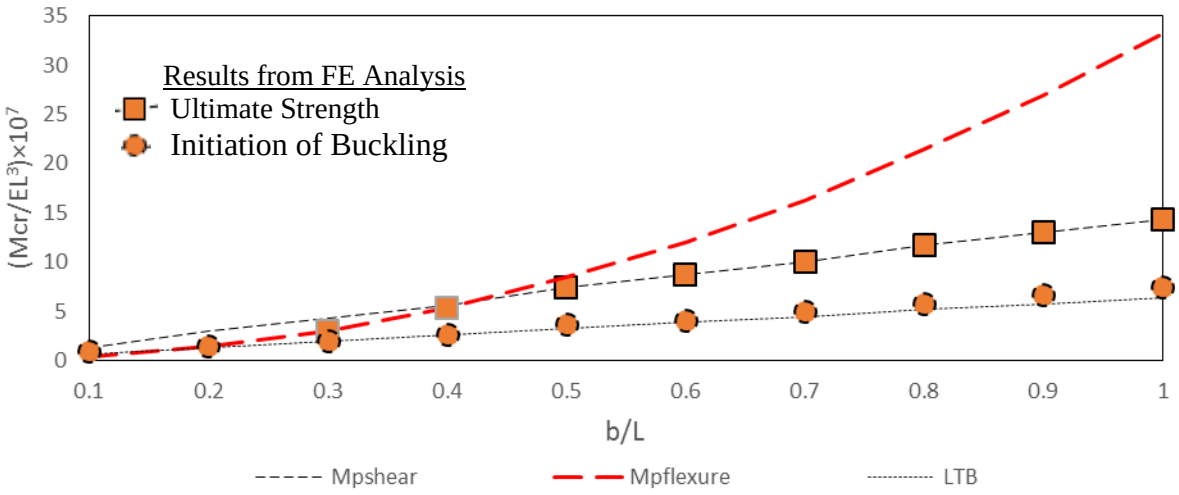

a) Butterfly link with a/b =0.33, t/L=0.01, and L=1m

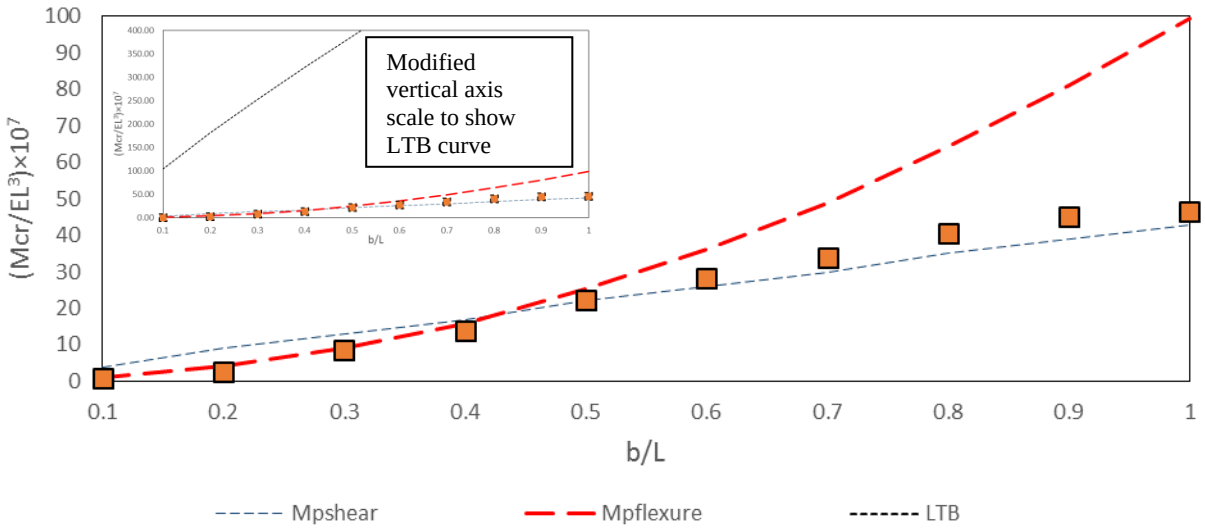

b) Butterfly link with a/b =0.33, t/L=0.03, and L=1m

Figure 8: Comparison of FE results to analytical equations for elastic and inelastic limit states

Fig. 8a, shows that the initiation of buckling in the inelastic FE models compared well with the moment predicted using the elastic differential equation. The ultimate moment strength of the links obtained from FE analysis compared well with the plastic strength equations in both Fig. 8a and Fig. 8b. In addition, the effect of thickness of the butterfly link on the lateral torsional buckling is demonstrated. As the thickness increases (Fig. 8b), the butterfly-shaped link would reach shear or flexure hinging capacity while elastic lateral torsional buckling governs for thinner links (Fig. 8a).

6. Conclusions

Butterfly-shaped structural fuse plates are a type of hysteretic damper used for seismic energy dissipation that consist of a set of butterfly-shaped links subjected to shear deformations. According to previous tests, these links are capable of substantial ductility and energy dissipation, but can also be prone to lateral torsional buckling. The governing differential equation for lateral torsional buckling of butterfly links was obtained and numerical solutions were presented. The results were compared with plastic moment capacity equations to examine which limit states would control for a typical range of links. Finite element models were constructed to verify the analytical results from the differential equation. The differential equation produced buckling moments that were on average within 5% of the FE model moments associated with buckling. Solution of the differential equation required significantly lower computational cost than computational simulation using FE analysis. In addition, the inelastic behavior of the links was investigated with FE models. Equations were provided to estimate the capacity of a link considering plastic shear yielding or plastic flexural hinging. Subsequently, the equations were verified against inelastic finite element models, and moments associated with inelastic lateral torsional buckling were compared to elastic lateral torsional buckling moments predicted by the differential equations.

Acknowledgments

This material is based upon the work supported by the National Science Foundation under Grant No. CMMI-1453960. Any opinions, findings, and conclusions or recommendations expressed in this material are those of the authors and do not necessarily reflect the views of the National Science Foundation or other sponsors.

References

Aschheim M., and Halterman A. (2002). "Reduced Web Section Beams: Phase One Experimental Findings And Design Implications." *7th U.S. national conference on earthquake engineering, Boston, Massachusetts*.

Asselin R.E, Fahnestock L.A., Abrams D.P. Robertson I.N., Ozaki R., and Mitsuyuki S. (2012)."Behavior and Design of Fuse-Based Hybrid Masonry Seismic Structural Systems", *15th WCEE Conference.*

Chan R., and Albermani F. (2008). "Experimental Study of Steel Slit Damper for Passive Energy Dissipation", *Engineering Structures*, 30 1058–1066.

C.Young W., and Budynas R. G. (2002)."Roarks Formulas for Stress and Strain." McGraw-Hill.

Farzampour A., Laman J. Mofid M. (2015). "Behavior Prediction of Corrugated Steel Plate Shear Walls with Openings", *Journal of Constructional Steel Research*, 114 258–268.

Ma X., Borchers E., Pena A., Krawinkler H., Billington S., and Deierlein G. (2011). "Design and Behavior of Steel Shear Plates with Opening as Energy Dissipating Fuses", *The John A. Blume Earthquake Engineering Center*. Report No. 173.

Martınez-Rueda, J.E. (2002). "On The Evolution of Energy Dissipation Devices for Seismic Design." *Earthquake Spectra*, 18 (2) 309-346.

Timoshenko, S., and Gere, J. M. (1961). "Theory of Elastic Stability". *New York: McGraw-Hill*.

Tsai K., Chen H., and Hong C. Su Y. (1993). "Design of Steel Triangular Plate Energy Absorbers for Seismic-Resistant Construction". *Earthquake Spectra*, 9 (3).

Vargas, R.E., and Bruneau, M. (2006). "Seismic Response and Design of Buildings with Metallic Structural Fuses." *Proceedings of the Fifth International Conference on Behaviour of Steel Structures in Seismic Areas (STESSA), August 14-17, Yokohama, Japan*, pp 99-103.

Whittaker, A. S., Bertero, V. V., Thompson, C. L., and Alonso, L. J. (1991). "Seismic Testing of Steel Plate Energy Dissipation Devices", *Earthquake Spectra*, 7 (4), 563–604